Monitoring Streambed Scour/Deposition Using Non-Sinusoidal Water Temperature Signals and During Flood Events

A Thesis

Presented in Partial Fulfillment of the Requirements for the

Degree of Master of Science

with a

Major in Civil Engineering

in the

College of Graduate Studies

University of Idaho

by

Timothy R. DeWeese

Major Professor: Daniele Tonina, Ph.D.

Committee Members: Ralph Budwig, Ph.D.; Charles Luce, Ph.D.

Department Administrator: Richard Nielson, Ph.D.

July, 2015

Authorization to Submit Thesis

This thesis of Timothy R. DeWeese, submitted for the degree of Master of Science in Civil Engineering and titled "Monitoring Streambed Scour/Deposition Using Non-Sinusoidal Water Temperature Signals and During Flood Events," has been reviewed in the final form. Permission, as indicated by the signatures and dates below, is now granted to submit final copies to the College of Graduate Studies for approval.

Major Professor: _____ Date: _____
Daniele Tonina, Ph.D.

Committee Members: _____ Date: _____
Ralph Budwig, Ph.D.

_____ Date: _____
Charles Luce, Ph.D.

Department Administrator: _____ Date: _____
Richard Nielson, Ph.D.

Abstract

Streambed erosion and deposition are inherent to river beds, and monitoring their evolution is important for ecological system management and instream infrastructure stability. The thermal scour-deposition chain (TSDC) is a novel tool capable of simultaneously monitoring scour and deposition, stream sediment thermal regime, and seepage velocity information, but previous research did not address non-sinusoidal temperature variations and natural flooding conditions. Laboratory tests show the TSDC is equally capable of measuring scour-deposition sequences and seepage velocity using sinusoidal and non-sinusoidal temperature signals under a range of seepage velocities. Application in a dam release stream during flood condition shows excellent match between surveyed and TSDC-monitored bed elevation changes and provides useful seepage velocity information even under very low temperature signal amplitudes. Future research should focus on improved techniques for temperature signal phase and amplitude extractions, as well as TSDC application to monitor scour at bridge piers and abutments.

Acknowledgements

There are a number of people and organizations to whom I owe my greatest appreciation. Without them, this work would not have been possible. I would like to thank my advisor, major professor, and mentor Dr. Daniele Tonina for his much needed guidance and patience through the entire process of writing research grants, experiment design, data collection and analysis, and completion of this thesis. He was available whenever I needed him, which cannot be easy given his busy schedule. Dr. Charles Luce provided much needed technical support when air bubbles were my nemesis and mathematical genius when data analyses went awry. The laboratory experiment would have been missing the critical sinusoidal (and non-sinusoidal) water temperature supply without the many hours of programming by John Berndt, with Bolen's Control House in Boise, Idaho. Bob Basham, our lab manager, helped keep experimental and field equipment design to manageable, constructible levels. Mohammad Sohrabi and Dr. Daniele Tonina toiled alongside me for hours, pounding those pesky temperature probes into the rocky streambed. Rohan Benjankar and Jeff Reeder assisted with field surveying and pebble counts. Dr. Jairo Hernandez at Boise State University called me during the summer following my undergrad work to be a research assistant. Prior to this call, I did not see research in my future. There are many folks at Boise State University that made completing my bachelor's degree possible. Thank you to them because without the B.S., grad school would of course not have been possible. I would like to thank the Hydro Research Foundation for providing the research award that funded my final year. Brenna Vaughn and Deborah Linke with the foundation work tirelessly to support students performing research in fields related to hydropower. Finally, I would like to thank the Idaho State Board of Education and Idaho Transportation Department for additional project funding.

I owe my deepest gratitude to my family, to whom I have dedicated this work. I started as a freshman at Boise State University in Civil Engineering six years ago and went straight into grad school at University of Idaho. To complete all of this work in six years in engineering is a difficult task and consumed much of my non-sleeping time every day and week. My wife endured many days of doing all of the family and household duties while I studied and researched. She was my rock, my motivator, and my shoulder to rest on when things got excessively stressful. And, last but not least, I thank my children. My children were the absolute biggest motivator of all. Many times I would look at them and realize I am doing all of this for them, to lead them and to leave them and their children a bright future full of life and beauty. My father taught me to leave it better than I found it. I have taken this to the full extent and am doing everything I can to leave the world a better place for my children and theirs.

Dedication

To my beautiful wife, Julie, I dedicate this work to you as a thank you for all of your much needed love and support throughout my college education. To my children Averi, Brady, and Jacob, you are our future. With hard work and dedication to a set of goals, you will do great things. To my mother and father, Sherry and Frank, thank you for instilling in me the drive and can't quit attitude it takes to accomplish a task of this magnitude.

Table of Contents

List of Figures

List of Tables

1.0 Introduction

Hydromorphological dynamicity is inherent to river beds and affects many hydrologic, geomorphic, and ecological processes within rivers (Gurnell et al., 2012; Knighton, 1998; Lytle and Poff, 2004; Richards et al., 2002). Research has addressed ecological impacts of anthropogenic stream channel modifications and associated sediment transport on fish habitat, benthic organisms, vegetation communities, and others (Newson and Newson, 2000). Among many human modifications, dams are one example that impacts all of these ecological categories (Graf, 2006; Knighton, 1998, pp. 307–312; Ligon et al., 1995; Petts and Gurnell, 2005). Adaptive management strategies have been implemented in attempt to reduce anthropogenic effects in water resource management (Ligon et al., 1995; Richter and Thomas, 2007). Streambed erosion (scour) and deposition also have important implications with hydraulic structures placed in rivers. Damage to thousands of bridges has been linked to bridge pier and abutment scour during high flow events (L.A. Arneson et al., 2012). Major programs have been established to predict and monitor bridge scour to reduce public safety risk and costly infrastructure loss (Mueller, 1998).

Monitoring channel dynamics is important for both ecological and engineering management of riverine systems (Maturana et al., 2014). Such information can aid in understanding bi-directional links among sediment transport and fish habitat, benthic organisms, and vegetation communities and is important for holistic management of river systems (Marion et al., 2014). Environmental flows from dams established to minimize negative impacts may result in scour-deposition events, intended or unintended (Richter and Thomas, 2007). Dam managers can utilize scour monitoring to quantify the significance of dam re-operation on the riverine

environment and for verification of desired results. Hydraulic structures susceptible to streambed scour and deposition can be monitored to provide warning of potential safety hazards and/or economically catastrophic events (Deng and Cai, 2009). Monitoring at bridge piers and abutments can be used in conjunction with scour prediction models to provide a complete system for hazard prevention during flood events.

Several methods have been reviewed for measuring erosion and deposition of stream beds (Cooper et al., 2000; Deng and Cai, 2009, pp. 129–131; Mueller, 1998; Nassif et al., 2002). A common and simple method for measuring erosion is the scour chain, which records maximum erosion during a high flow period and potential subsequent deposition. This method is time consuming, difficult to install and remove, and provides no timing of measured erosion and deposition. Other methods have been explored including the magnetic sliding collar, piezoelectric probes, heat dissipation gauges, photo-electric cells, and conductance probes. Sonar, radar, time-domain reflectometry, and fiber Bragg grating sensors have also been implemented to monitor erosion and deposition continuously (Manzoni et al., 2011). Limitations of these technologies include deployment costs and difficulty deploying large sensor networks to obtain a distributed erosion-deposition pattern.

A newly developed method uses temperature as a tracer to monitor streambed erosion and deposition (Gariglio et al., 2013; Luce et al., 2013; Tonina et al., 2014). This method, referred to as the thermal scour-deposition chain (TSDC), is similar to a technique used for measuring sediment pore water flux associated with surface water–groundwater exchange and hyporheic flows (Gariglio et al., 2013; Hatch et al., 2006; Keery et al., 2007; Lautz, 2012, 2010; Rau et al., 2012; Stallman, 1965). Previous research shows that this new method has several advantages over existing methods: (1) it uses proven, robust and economical temperature

sensing technology; and (2) it can simultaneously be used to quantify stream sediment thermal regime, thermal properties, and sediment seepage velocity. Such advantages make the TSDC not only a very useful scour monitoring tool but also a tool for improving understanding of ecological implications due to dam operation and environmental flow regimes.

The TSDC was previously tested under limited imposed scour and deposition sequences with well-defined sinusoidal daily temperature oscillations, lack of vertical thermal gradients, and under low, near stationary surface flows (Tonina et al., 2014). While previous results showed reasonable proof of concept under this scenario, the method should be tested in natural systems where scour and deposition occur in association with changing discharge. Furthermore, previous research has indicated uncertainty may arise when using the temperature methods to analyze streambed water flux due to non-sinusoidal signals of temperature and vertical thermal gradients (Lautz, 2010). Because TSDC uses the same mathematical framework and imposed boundary conditions, sinusoidal forcing and zero-thermal gradient at the two ends of the domain respectively, this research expects to detect similar inaccuracies when using non-sinusoidal temperature signals for measuring erosion and deposition with the TSDC. Consequently, this study was designed to address two fundamental questions regarding the applicability of the TSDC: (1) Will a non-sinusoidal temperature signal provide results similar to the sinusoidal signals? and (2) How well does the method perform in a natural system during high flow events?

To address question 1, a laboratory sediment tank was designed, which mimics natural stream processes, including a cyclic surface water temperature signal, sediment vertical pore water flux, and scour/deposition sequences. A programmable logic controller (PLC) controls the surface water temperature, imposing sinusoidal and sawtooth (non-sinusoidal) wave signals.

The advantages of the laboratory sediment tank are the possibility to impose erosion and deposition sequences accurately and precisely, as well as vertical seepage fluxes and to avoid outside influences on errors in physical measurement (e.g. animals scouring the bed).

A field study was performed to address question 2. The South Fork Boise River (SFBR) was selected, 2 miles downstream of Anderson Ranch Dam (Figure 1). This site was chosen because of (1) recent massive alluvial deposits from tributaries and (2) planned flow regime to flush the alluvial deposits, which would enhance the opportunity to monitor changes of bed elevation. While high flows are not due to natural flooding, scour/deposition sequences that occur are natural and linked to dam operation and water resource management strategies.

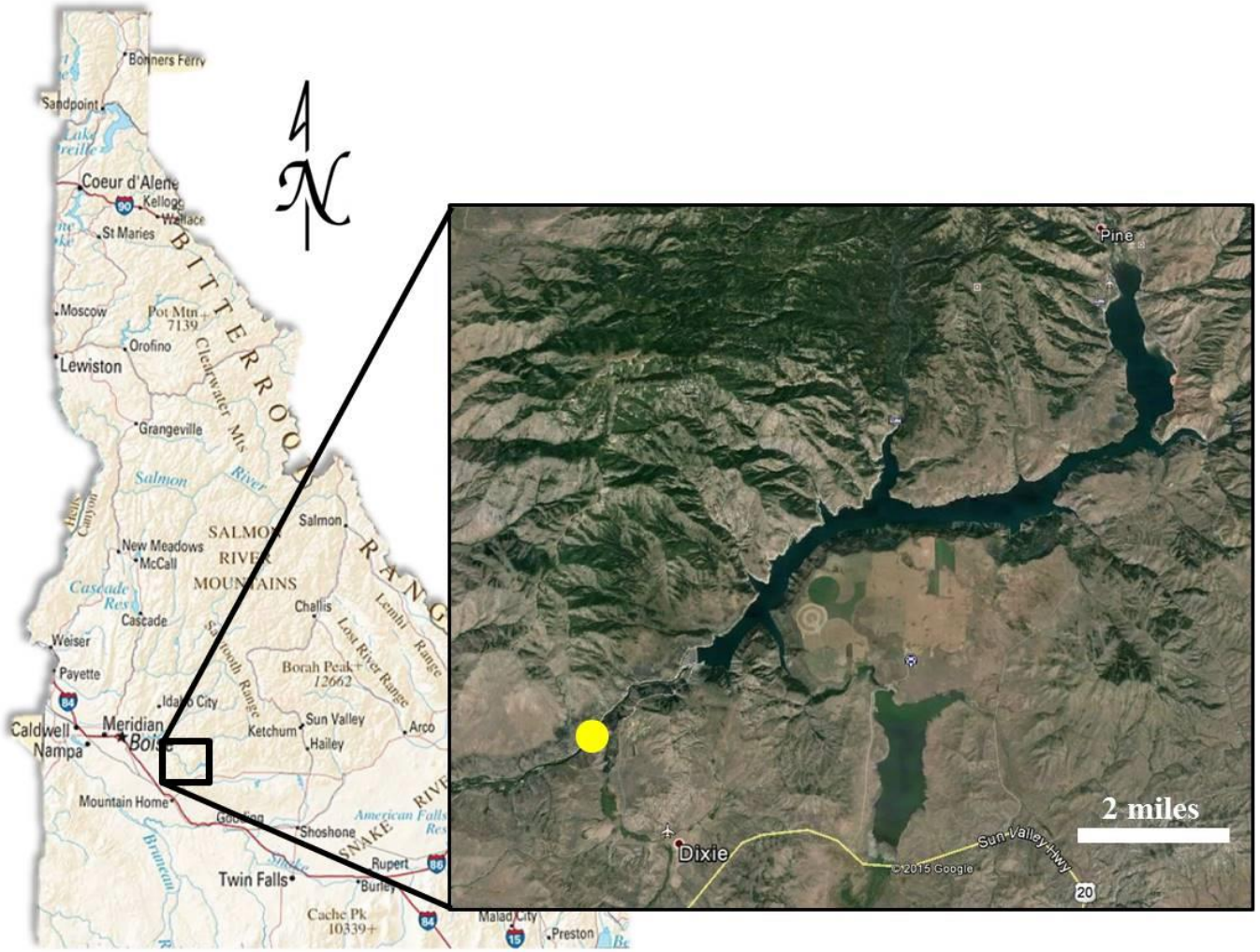

Figure 1: Field study site, located 2 miles downstream of Anderson Ranch Dam on the South Fork Boise River, Idaho, USA.

2.0 Methods

2.1 Theory

Sediment elevation changes are quantified using a mathematical method based upon one-dimensional advection and diffusion of temperature (Luce et al., 2013; Tonina et al., 2014), where phase, ϕ, and amplitude, A, of cyclic temperature signals from paired temperature sensors in the surface water and within the streambed sediment are analyzed (equations 1-3):

$$\eta = \frac{-\ln\left(\frac{A_2}{A_1}\right)}{\phi_2 - \phi_1} = \frac{-\ln(A_r)}{\Delta\phi} \quad \textbf{(1)}$$

$$\kappa_e = \frac{\omega \Delta z^2}{\Delta\phi^2}\frac{\eta}{1+\eta^2} \quad \textbf{(2)}$$

$$\Delta z = \Delta\phi\sqrt{\frac{\kappa_e}{\omega}\left(\eta + \frac{1}{\eta}\right)} \quad \textbf{(3)}$$

where η is a dimensionless number relating the natural logarithm of the amplitude ratio, $A_r = \frac{A_2}{A_1}$, to the phase difference between paired temperature signals, $\Delta\phi$. $\omega = \frac{2\pi}{T}$, is the expected angular frequency and T is the period of the temperature signal being analyzed. Calculation of sediment thickness between temperature sensors, Δz, allows quantification of bed elevation changes over time. Effective thermal diffusivity, κ_e, is a thermal property of the sediment and pore-water matrix and is calculated from the temperature time series obtained during an intitial, steady state elevation of the bed where Δz is known and constant. This calculation of κ_e is different from previous methods (Constantz, 1998; Hatch et al., 2006; Keery et al., 2007; Lautz, 2012; Swanson and Cardenas, 2010), which require an estimated value of κ_e. Once known, κ_e should remain unchanged through the experiment, thus the value

is held constant, and Δz over time is calculated. Bed elevations are then calculated by summing Δz and respective temperature sensor constant elevations.

Seepage velocities, i.e., Darcy velocities, can be calculated at each location once κ_e is known. Luce et al. (2013) provide one option for calculating advective thermal velocity independent of depth:

$$v_t = \frac{z_d \omega}{\sqrt{2\eta}} \frac{1-\eta^2}{\sqrt{1+\eta^2}} \quad \textbf{(4)}$$

where z_d is the diurnal damping depth and is related to κ_e:

$$z_d = \sqrt{\frac{\kappa_e}{\omega}} \quad \textbf{(5)}$$

Darcian velocity relates to advective thermal velocity with

$$v = v_t \gamma \quad \textbf{(6)}$$

where

$$\gamma = \frac{\rho_m c_m}{\rho_w c_w} \quad \textbf{(7)}$$

ρ refers to density and c to specific heat capacity. Subscripts *w* and *m* refer to the water and the sediment pore-water matrix, respectively. Seepage velocity can be calculated by dividing the Darcian velocity by the sediment effective porosity. Equations 4 through 7 can be combined to form one equation for seepage velocity related to κ_e, which is used throughout the presented analyses:

$$v = \gamma \sqrt{\frac{\kappa_e \omega}{\eta}} \frac{1-\eta^2}{\sqrt{1+\eta^2}} \quad \textbf{(8)}$$

The analytical solutions behind this mathematical method are similar to those used by researchers to quantify streambed seepage flux (Hatch et al., 2006; Keery et al., 2007; Lautz, 2012, 2010; Rau et al., 2012; Stallman, 1965). Multiple assumptions behind the analytical solution have been reported, including (1) sinusoidal temperature signal in the stream surface water, (2) zero vertical gradient of mean temperature with depth in the streambed, and (3) equal streambed pore-water and adjacent sediment temperatures. Research has demonstrated increased error in seepage velocity calculations associated with violations of assumptions 1 and 2 (Lautz, 2010), and excellent results (<1% error) when ideal sinusoidal temperature signals are analyzed under low or no seepage flow conditions. Research presented in this paper tests capability of the TSDC to monitor streambed scour and deposition with presence of violations to these assumptions.

The equations and the signal analysis were coded in the open source statistical computing environment, R. Numerical analysis uses a discrete Fourier transform (DFT) to extract phase and amplitude from cyclical temperature time series and combines these extractions with equations 1 through 8 to obtain bed elevation and velocity data. Bed elevation and velocity calculations use only measured temperature data and require no parameterizations.

2.2 Lab Experiment

To test the TSDC applicability with non-sinusoidal temperature signals in the laboratory, a small sediment tank was designed to mimic natural streambed processes. These processes include: cyclic temperature surface water flow, a sand stream bed with seepage velocity in both upwelling or downwelling conditions, and scour-deposition sequences. Only

downwelling experiments are presented in this work. A simple sketch of the laboratory experiment is provided in Figure 2.

The 40 cm square, 80 cm tall sediment tank is constructed of 3/8 inch clear cast acrylic sheeting. The tank bottom has two layers, the first of which, with respect to water flowing down through the tank, is a grid of 100, 3/16" holes that help maintain vertical flow streamlines through the above sediment matrix. Five centimeters below the grid and 5 cm above the tank wall bottom is the tank bottom, which has a centered hose fitting for connection of the downwelling plumbing. This section between the grid and tank bottom is void of sediment and allows downwelling water to be collected with minimal effect on flow lines through the sediment. Clear poly (3/8" OD, 1/4" ID) tubing was selected for the hydraulic system, and flow rate control is accomplished via constant head tanks for supply and upwelling/downwelling flows.

The surface water supply head tank is fed by the outlet of a controlled temperature mixing valve, and constant head is maintained through a 1 inch PVC stand pipe drain. Sediment tank surface water, which mimics the stream flow, flows from the supply head tank, through the surface water tank and out through a stand pipe drain. Downwelling pore water flow is induced via a constant head difference from surface water in the sediment tank to drain outlet. A sand bed is used in the sediment tank. Grain sizes range from 0.178 to 2 mm and median grain size, d_{50}, of 1.16 mm and total initial sediment depth of 45 cm.

Cyclic source water (i.e. surface water) temperature control is accomplished using an Omron CP1L-EL20DR-D programmable logic controller (PLC), which operates a Honeywell MN7505 temperature control actuator on a Honeywell VBN3 mechanical mixing valve. Temperature control parameters including mean, amplitude, period, and signal type for the

PLC are selectable through a programmable graphical user interface (GUI) (using Indu-Soft Web Studio (http://www.indusoft.com/Products-Downloads/HMI-Software/InduSoft-Web-Studio). Several PID parameters were adjusted to control the response to feedback temperature, which is provided with an HSRTD-3-100-A-180-E, hermetically sealed waterproof resistance temperature detector (RTD) from Omega Engineering (http://www.omega.com/pptst/HSRTD.html). Hot water is provided to the inlet of the mixing valve via a pump in the heated (using a standard submersible bucket heater) recirculation water tank that collects outlet water from the system, excluding downwelling flow. Cold water is pumped to the mixing valve from the laboratory water reservoir pool. A small pump is also placed within the surface water of the sediment tank to ensure the surface water temperature is well-mixed and to avoid thermal water stratification within the surface water in the sediment tank.

The temperature probe placed in the center of the sediment tank is constructed with eleven Dallas Semiconductor waterproof digital temperature sensors (DS18B20) inserted along an ultra-high molecular weight plastic strip at 5 cm intervals. These sensors provide 0.625 degree Celsius resolution and 750 millisecond sampling capability. An Arduino microcontroller based data logging system was selected for its ability to communicate via serial data with the temperature sensors and potentially add telemetry in the future. Temperature data is logged at 30 second intervals.

A weather station tipping bucket is used to measure the average downwelling flux through the sediment. The device collects water from the downwelling outflow tube and tips at a calibrated average 9.45 mL. An additional Arduino microcontroller is combined with a micro-SD data logging shield to record the tip count. Downwelling flow rate is converted to Darcy

velocity by dividing the flow rate by the sediment tank horizontal cross-sectional area of 1600 cm^2 (40 cm x 40 cm).

Four sediment tank experiments consist of a sequence of manually imposed scour and deposition events. Variations among experiments A, B, C, and D are shown in Table 1. Downwelling flow rate is held constant for each experiment and is similar for the respective low and high velocity settings. Surface water temperature signal parameters are set to a period of 2 hours and peak to peak amplitude of 8 degrees Celsius for experiments A, B, and C and 4 degrees Celsius for experiment D. Sinusoidal and sawtooth signal types are implemented, separately, to compare results (Figure 3). Scour and deposition sequences of approximately 5 cm bed elevation changes are manually imposed by scooping sand and leveling with a small piece of wood. Bed elevation is measured based upon a datum elevation set at the top of the tank of 100 cm. The distance to the bed is measured from the datum using a screw fixture reaching down from the top of the tank to the top of the bed particles at the center of the bed where the probe is located. The length of this fixture is then measured to the nearest 0.01 cm, and the value is subtracted from the 100 cm datum to obtain the bed elevation. The entire bed elevation is adjusted to +/- 1 mm of this measurement to avoid any spatial bed elevation variation influence on results.

Table 1: Laboratory sediment tank experiment velocity, signal type, and temperature signal amplitude settings for experiments A, B, C, and D.

Experiment	Downwelling velocity (cm/s)	Signal type	Amplitude (°C)
A	0.00022	Sinusoid	8
B	0.0017	Sinusoid	8
C	0.00027	Sawtooth	8
D	0.0017	Sawtooth	4

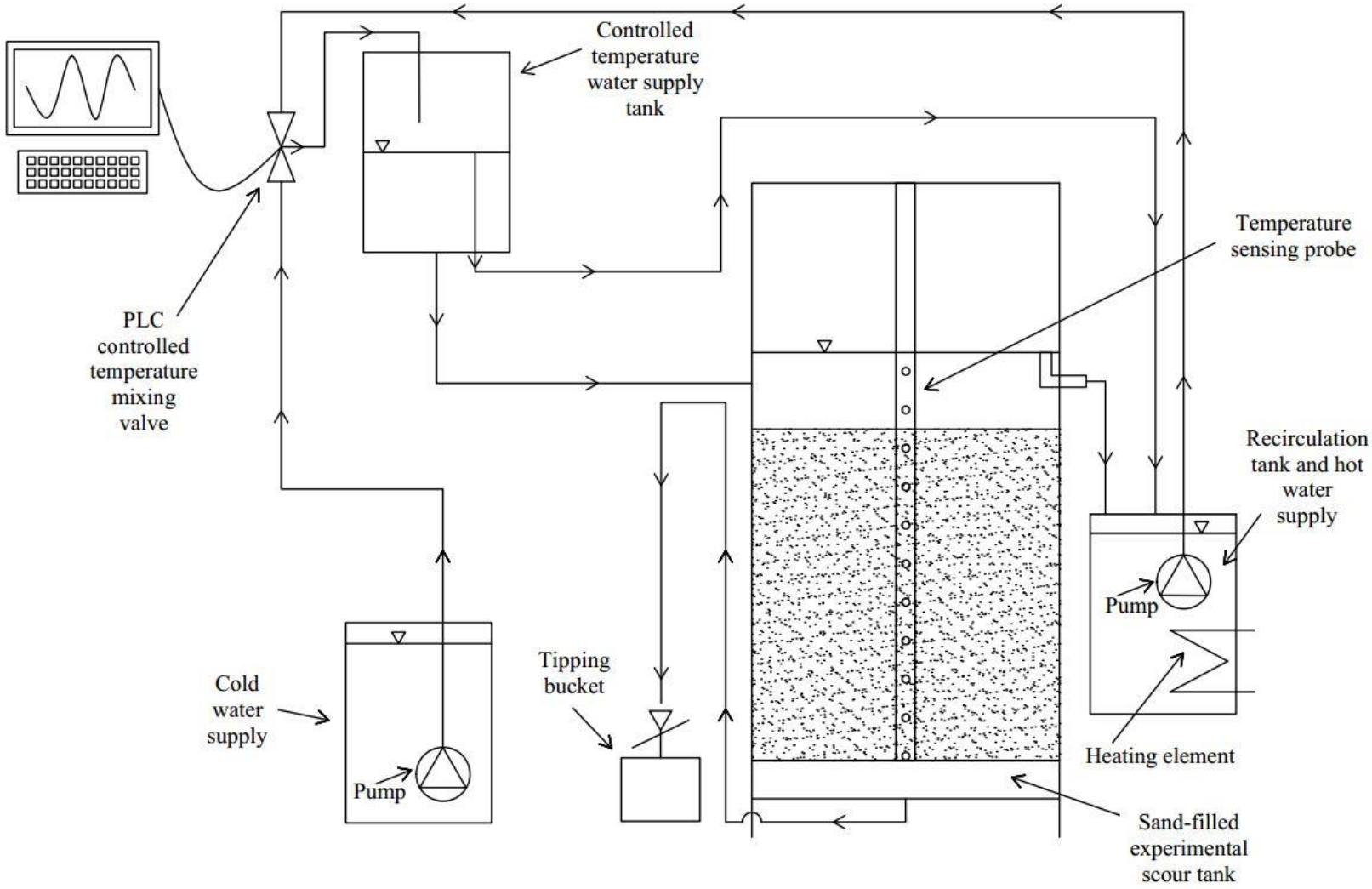

Figure 2: Sketch of laboratory experiment.

Scour/deposition events are imposed approximately every 24 hours or 12 cycle periods, and the time of the event is recorded in seconds from the beginning of the experiment. These data are used to create plots of the actual bed elevation with time to compare with the calculated result from each representative temperature sensor. With the goal to compare results from a sinusoidal versus saw tooth temperature signal, each experiment is repeated for the sinusoidal and saw tooth signal types. As well, there was interest in testing the method under both near zero and normal to high downwelling seepage velocity for a natural system to verify TSDC applicability in a range of velocities.

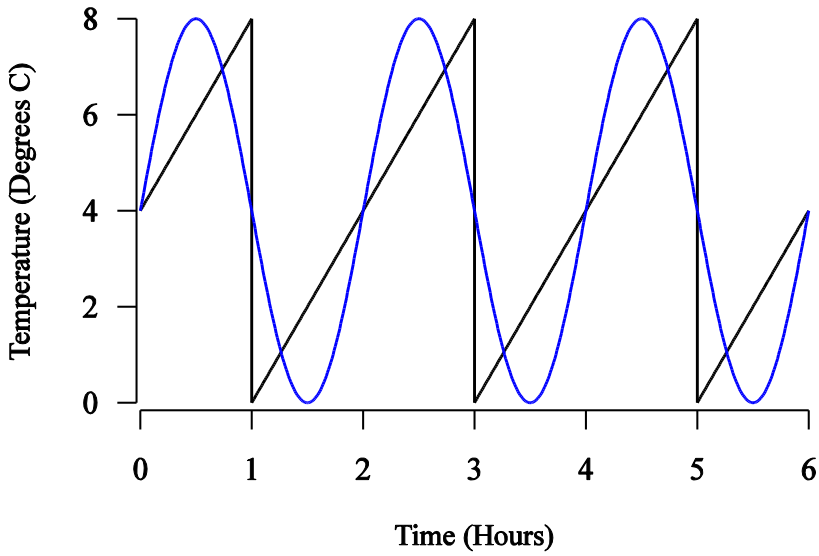

Figure 3: Imposed laboratory surface water temperature signals. Experiments A and B used a sinusoid signal (blue), and experiments C and D used a sawtooth signal (black), both have same wavelength.

2.3 Field Study Site

UHMW (Ultra High Molecular Weight) plastic tube houses the same DS18B20 temperature sensors used in the laboratory. The 1 inch long sensors are placed at a 45 degree angle to allow a smaller diameter tube. Exact sensor locations along the probe are referenced using the unique serial address of each individual sensor. The three wires from each sensor are

connected in a star network, allowing one three wire sleeved bundle to exit the top of the probe with a connector for connection to a data logger. This connector provides the advantage to connect the probe to an attached data logger or to run longer wires and connect multiple probes to one central data logger. A 60 degree angled aluminum cone drive tip is inserted and pinned in the bottom of the probe and is larger in diameter at the probe/tip interface, allowing for driving and anchoring the probe. The anchor ensures the probe will not uplift or float out of the sediments during deployment and during scour events, assuming scour is not so deep to remove the probe entirely. An open source Arduino based microcontroller is used for data logging onto a micro SD card. It is powered with AA, alkaline batteries and is placed inside a waterproof housing, constructed with 1 ½ inch PVC fittings and pipes.

Installation in the field can be challenging and involves driving the probe into the streambed using a 2 ½ inch diameter cast iron pipe and a large post hammer. The drive tip fits snuggly just inside and against the bottom end of the driver and is placed with the probe inserted in the pipe before driving the assembly vertically down into the stream bed with a post hammer. The driver is then carefully pulled up, leaving the installed probe in the bed. The data logger is then connected to the probe with the waterproof connector and placed on top of the probe using the threaded connection. Excess wire is placed within a storage cavity in the data logger housing during deployment.

Field temperature probes were deployed on August 6, 2014 in the South Fork Boise River (SFBR) (Figure 4) to monitor streambed scour/deposition associated with dam release flows from the upstream Anderson Ranch Dam. Several tributaries to the SFBR deposited major alluvial sediments into the river in 2013 following wildfires in the area. One of the largest debris fans was selected for scour monitoring due to the high probability of changes in

streambed elevation due to the loose arrangement of the sediment. The U.S. Bureau of Reclamation (USBR) manages the dam and planned a high flow release of 68 m^3s^{-1} (hereafter referred to as flood) for the period from August 18 through 27 to remove fine sediments delivered by the debris fans. Grain size distributions for the streambed before and after the flushing flow (i.e. flood) are shown in Figure 5 for the selected debris fan.

Two of the aforementioned temperature probes were installed. In addition, two probes constructed of Hobo Tidbit sensors in PVC pipe, similar to the design presented in the work of Tonina et al. (2014), were used at intermediate locations of the two other probes. To collect water surface temperature, one additional, single Hobo Tidbit sensor was placed in the surface water where no scour or deposition was expected. Data from each temperature sensor was collected and recorded at fifteen minute intervals. Probe locations and initial bed elevations relative to the probe and a control point were surveyed using an engineering level. The four locations are labeled 1, 2, 3, and 4, starting at the upstream end of the debris fan toward the downstream end, respectively. The probes were deployed until September 29, at which point the probes were no longer submerged. Final bed elevations relative to each probe were measured using a ruler prior to removal. To evaluate scour/deposition, each probe location is assigned an initial bed elevation of 0 cm, thus scour events are represented by negative values and deposition with positive values. Bed elevation change is tracked by measuring the distance from the top of the probe to the bed before and after the high flow event. Increase in the distance indicates scour occurred (negative bed elevation), and decrease in the distance indicates deposition occurred (positive bed elevation). No additional measurements were possible during the flood period due to safety.

Figure 4: Left: South Fork Boise River study site showing the debris flow that added sediment to the channel, with approximate thermal scour/ deposition chain installation locations 1, 2, 3, 4. (Photo used with permission from the USDA, Boise National Forest); Middle: Field temperature probe; Right: Temperature probe installed with data logger.

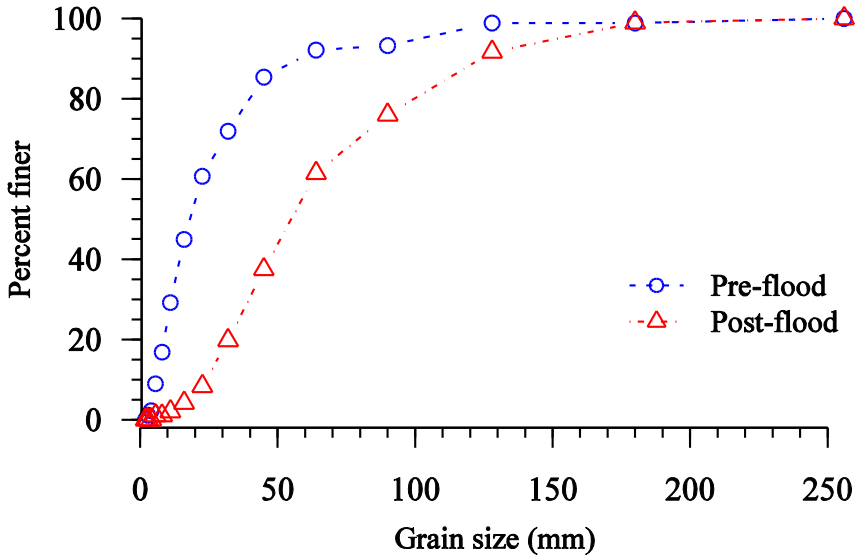

Figure 5: Pre-flood (blue) and post-flood (red) grain size distribution at South Fork Boise River locations 1 and 2. Locations 3 and 4 did not experience significant change in grain size distribution due to little scour or deposition and their grain size distribution remained similar to the pre-flood condition.

3.0 Results

3.1 Lab Experiment

Temperature signal penetration depth is dependent upon several mechanisms, including diffusion, dispersion, conduction through water and solids, and advection. Advection transports the periodic signal unaltered, whereas conduction and dispersion attenuate the signal amplitude to zero. Sensors below the depth where the oscillations are removed and constant temperature is established are not used to calculate changes in streambed elevation (Figure 6a and c). Similarly, sensors that become exposed to the surface water during scour cannot be used, because amplitude ratio is 1 and phase differences are zero, thus there is no solution to the equations.

A good indicator of temperature sensors from which useful data may be obtained is the plot of phase versus depth (Figure 6b and d). In the range of negative sediment depth (i.e. in the surface water), phases should be equal, assuming the surface water is well mixed by turbulence. Phase change is linear with depth where sensors are buried and a signal is present, and the linear relationship is no longer present when the signal amplitude is not detectable. Useful data is available from sensors in the linear region (between the dashed lines in Figure 6b and d). Figure 6b shows sensors 1-3 have the same phase and are all in the water at the time of the plot. Figure 6d shows phase with depth during a deposition period in experiment A where the surface water mixing pump was not operating. Note the different phase values above the bed (0cm) that are calculated from temperature data from sensors 1 and 2, both in the surface water. This is an indication of stratification of surface water temperature.

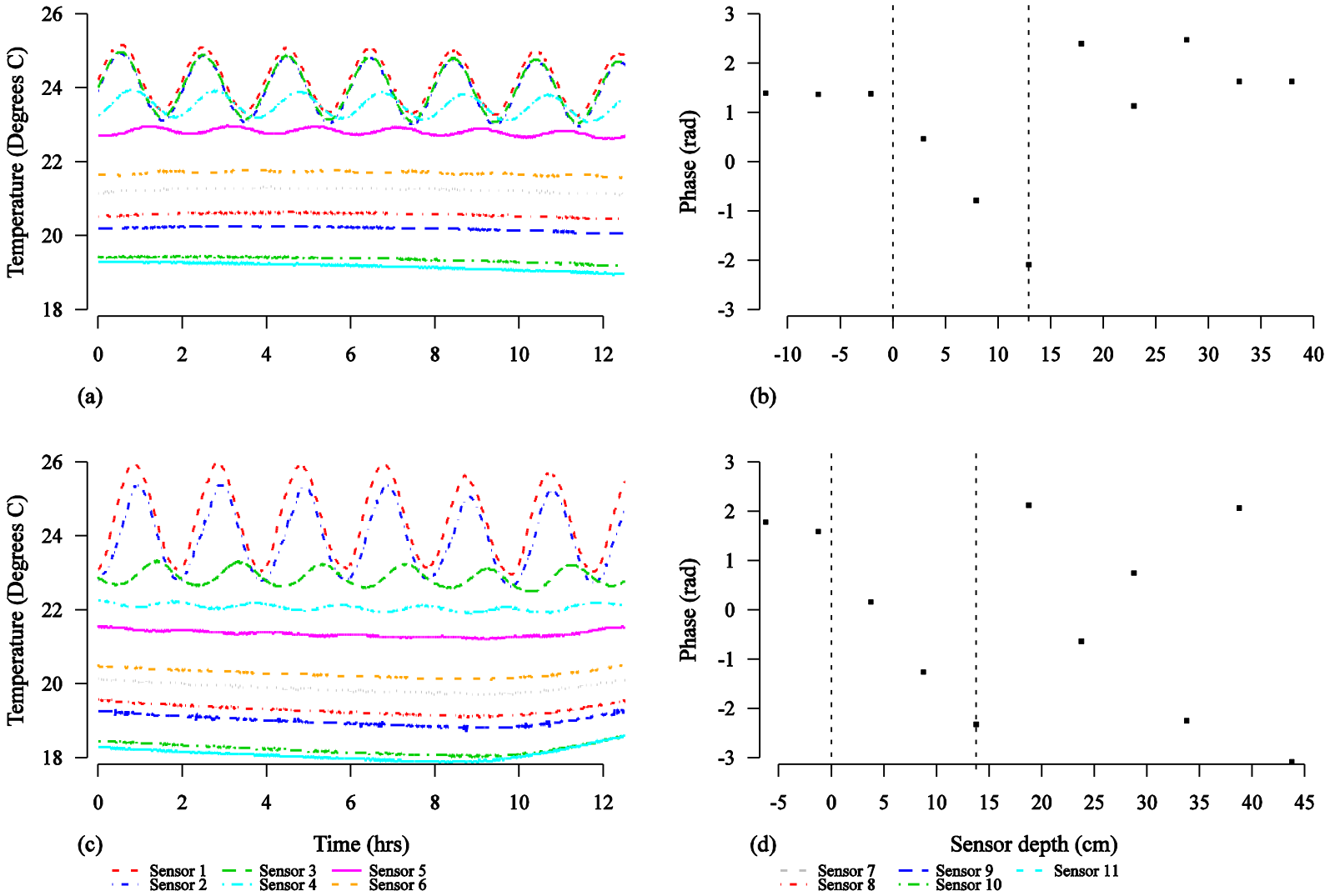

Figure 6: Plots from experiment A. (a) Example of measured sediment tank temperatures during a scour period. (b) Phase with depth from data in 4a. (c) Example of measured sediment tank temperatures during a deposition period. (d) Phase with depth from data in 4c. Vertical dashed lines in b and d indicate range of depth where data is useful, starting at the bed location of 0 cm.

From the plots, temperature signals measured at sensor locations 4 and 5 consistently are within the sediment and have strong enough cyclic signals for analysis, thus are used for the remainder of the analyses for both the sinusoidal and saw tooth signal experiments.

For these sensor locations and each respective experiment, thermal diffusivities calculated from the period of data prior to the first scour event average 0.0058 cm^2s^{-1} and range from 0.0051 to 0.0061 cm^2s^{-1}, with lower values calculated from sensor 4 in all experiments. For best results, it was necessary to use thermal diffusivities specific to depth location, opposed to a spatial average over the depth of the bed.

Time series plots of the imposed and calculated bed elevations are shown in Figure 7. Figure 7a shows a mid-experiment deposition period with poor elevation results. This result is from the time period when the surface water mixing pump stopped working (Figure 6c and d). All other scour-deposition sequences match well with the imposed values; however bed scour predictions occur early compared to the timing of scour. Errors in calculated scour are reported as Root Mean Squared Error (RMSE) in Table 2, excluding time periods of early scour prediction and no surface water mixing. Experiments A and C compare very well and show no apparent difference in scour results among signal types. Experiments B and D have similar results, with minor increased RMSE for D. In all experiments, scours calculated show increase in RMSE with increasing depth of temperature measurement.

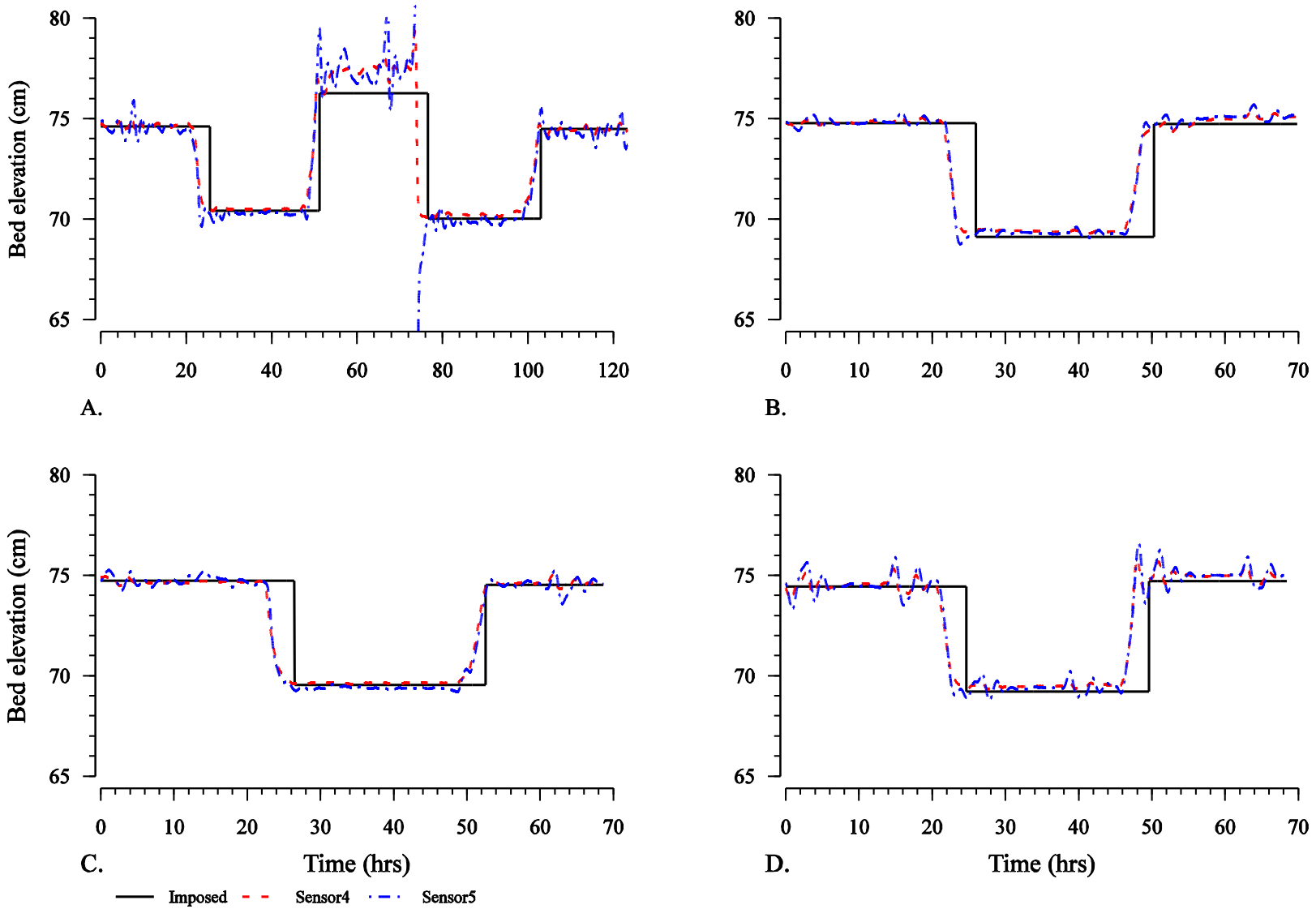

Figure 7: Sediment tank bed elevation over time for experiments A, B, C, and D. Data is only shown as calculated from sensors 4 and 5 for clarity.

Table 2: Bed elevation RMSE.

Sensor location	Experiment bed elevation RMSE (cm)			
	A	B	C	D
4	0.35	0.29	0.34	0.42
5	0.40	0.30	0.41	0.52
6	-	0.51	-	0.78
7	-	0.76	-	1.04
8	-	0.98	-	-
9	-	1.19	-	-

Figure 8 shows seepage velocities from each laboratory experiment. Calculated velocities have some noise but vary around a nearly constant mean throughout the entire experiment. Comparing experiments A to C and B to D, there is no apparent difference in results among signal types. Large spikes in calculated velocities occurred at timing of manual scour/deposition events. Shaded regions indicate period of scour (i.e. scour, followed by deposition). Percent error for calculated velocities compared to the imposed velocities is high for the low velocity experiments and low for the high velocity experiments (Table 3). The difference between imposed and calculated velocity increases with depth, especially in the high velocity experiments, where depth of signal penetration is greater.

Table 3: Mean calculated velocities and percent error for each sensor in experiments A, B, C, and D.

Sensor location	Mean calculated velocity (cm/s)				Velocity percent error			
	A	B	C	D	A	B	C	D
4	4.66E-05	1.20E-03	9.94E-05	1.23E-03	77%	28%	63%	27%
5	6.71E-05	1.38E-03	1.36E-04	1.38E-03	65%	19%	48%	19%
6	-	1.44E-03	-	1.44E-03	-	15%	-	15%
7	-	1.49E-03	-	1.48E-03	-	12%	-	13%
8	-	1.52E-03	-	-	-	10%	-	-
9	-	1.52E-03	-	-	-	10%	-	-

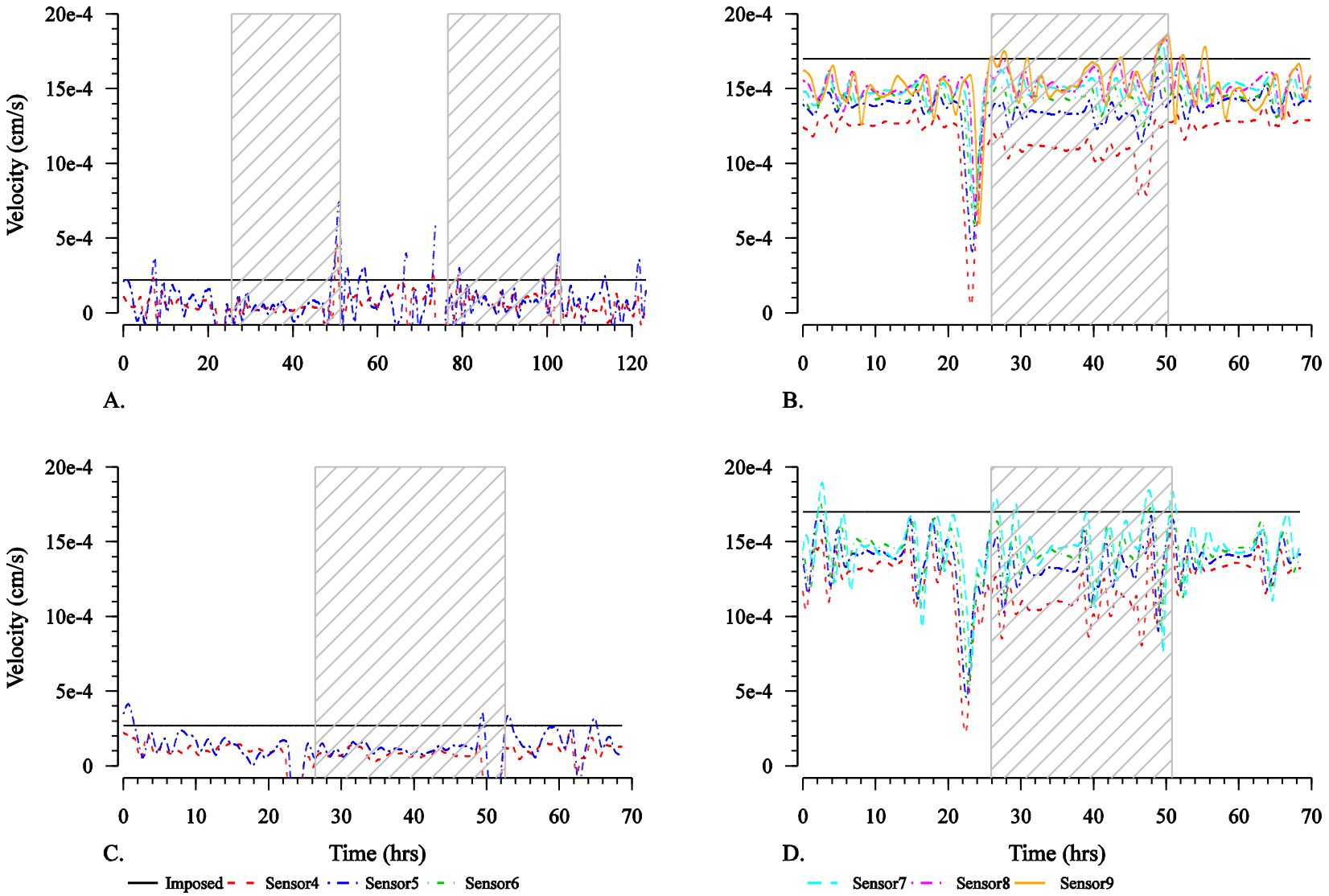

Figure 8: Laboratory experiment calculated and imposed velocities. Shaded regions indicate time period of scour shown in Figure 7.

3.2 Field Study Site

Figure 9 provides the measured temperature profile for the field temperature probe at location 1. Temperature profiles from the other locations are similar. Note the highest amplitude of measured temperature signal of approximately 1 degree C in the surface water for sensor 1 and amplitude of approximately 0.2 degrees C for sensor 3, 30 cm deep in the streambed. Low amplitude temperature signals can lead to noisy results of scour, deposition, and seepage velocity. Further, notice the gradient of mean temperature with sediment depth and non-sinusoidal temperature signals. These violations of the reported assumptions behind the method may lead to inaccurate bed elevation calculations.

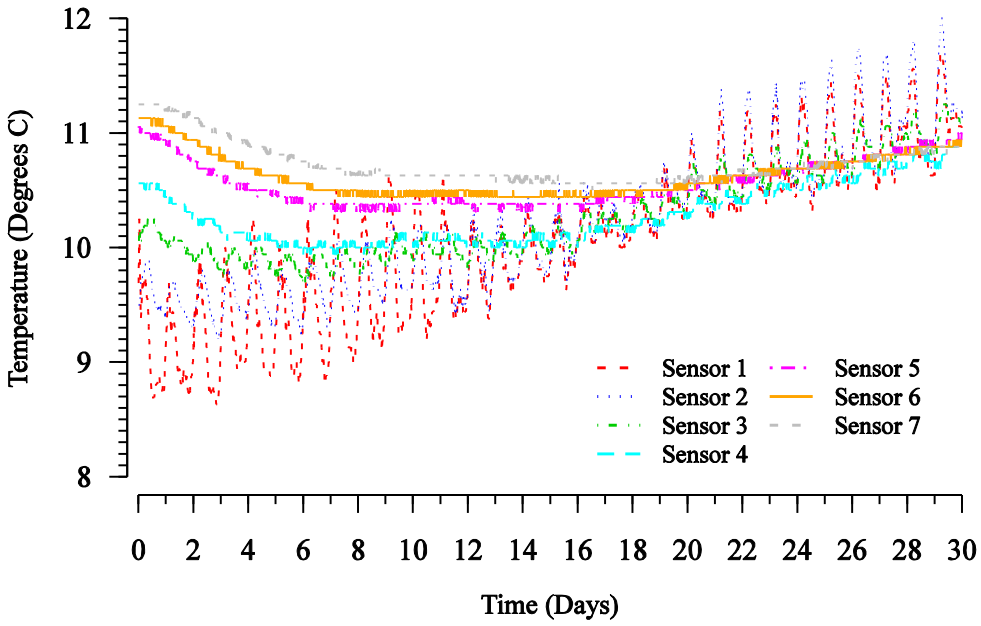

Figure 9: Temperature profile measured in the South Fork Boise River at location 1 for the submerged deployment period. Sensor 1 is at the surface water/sediment interface, and increasing sensor number represents increased sediment depth in 15 cm increments.

As with laboratory calculations, to provide κ_e for field scour/deposition and seepage velocity calculations, temperature data from each respective sensor was paired with sensor 1 (i.e. surface water sensor) data to obtain η in equation 1 and subsequently κ_e (thermal diffusivity)

from equation 2. The value of κ_e obtained by this surface water sensor pairing method can be used to calculate scour/deposition and seepage flux for each respective sensor depth location with potentially higher accuracy than a single average κ_e when spatial variation is present. For the latter, spatial values can be averaged to provide one κ_e value for the entire depth of sediment over the probe location depth. Temperature data from adjacent temperature sensors may also be paired to obtain κ_e and is used here to verify sediment did not move. Significant changes in κ_e can indicate sediment movement due to changing sediment thickness between sensors.

Calculated κ_e values for each probe location are provided in Table 4, including results calculated from paired adjacent sensors before and after flood flow and from each respective sensor paired to the surface water sensor. For the period prior to the flood flow, amplitude of the temperature signals from sensor 4 and deeper were too low to obtain results for κ_e at any of the four locations. After flood and associated scour events at locations 1 and 2, the temperature signal from sensor 4 was strong enough to obtain results, but sensor 2 no longer provided results as it was in the surface water. The paired adjacent sensor results were used to verify sediment did not move in these locations. Locations 3 and 4 provide very similar results before and after scour suggesting no sediment movement at these elevations along the temperature probe. At locations 1 and 2, values for sensor 4 after scour are similar to those at sensor 3 before scour, indicating that sediment between sensors 3 and 4 did not move, while some sediment between sensors 2 and 3 was scoured.

Table 4: Calculated effective thermal diffusivity, κ_e ($cm^2\ s^{-1}$), for each probe location. Adjacent pairs are comprised of the listed sensor and the sensor directly above it and provide vertical variability of κ_e. Sensors paired to the surface average κ_e from the respective sensor location to the water-sediment interface.

Field location	1	2	3	4
Adjacent sensor pairs pre-flood				
Sensor 2	0.0189	0.0159	0.0148	0.0077
Sensor 3	0.0067	0.0089	0.0062	0.0065
Adjacent sensor pairs post-flood				
Sensor 2	-	-	0.0336	0.0074
Sensor 3	0.0131	0.0247	0.0051	0.0062
Sensor 4	0.0069	0.0094	-	-
Paired to surface water sensor				
Sensor 2	0.0189	0.0159	0.0148	0.0079
Sensor 3	0.0105	0.0187	0.0078	0.0075
Mean of surface pairings	0.0147	0.0173	0.0113	0.0077

Figure 10 shows the streambed elevation changes calculated from the temperature data at each of the four probe locations in the SFBR, along with the pre-flood measured bed, post-flood measured bed, and post-flood calculated average bed. The last is the mean of the calculated bed elevation during post-flood period of data relative to the initial bed elevation of 0 cm at each location. Bed elevations relative to each probe were measured after installation using an engineering level and after flow recession using a ruler. For each plot, the dam release hydrograph is shown on the secondary axis in blue. Table 5 provides comparison of actual measured bed change and calculated change. Bed elevation change was also calculated using the surface-paired mean thermal diffusivities from Table 4 (i.e. one value of κ_e), and all of the values were within 1 cm of the calculated bed changes shown in Table 5.

Table 5: Measured and mean calculated streambed elevation changes and associated absolute error.

Field location	1	2	3	4
Measured bed change (cm)	-17.5	-30	-4.6	1
Mean calculated bed change (cm)	-18.80	-38.90	-6.9	1.7
Absolute Error (cm)	1.30	8.90	2.30	0.70

Stream sediment seepage velocities were calculated for each probe location (Figure 11). At locations 3 and 4, measured seepage velocities are near zero and have little noticeable change throughout the installation period. However, there is some noticeable increase in upwelling velocities (negative indicates upward velocity) at locations 1 and 2 during the high flow period and continuing after high flow subsided. Location 2 also appears to have some seepage velocity that is a function of streamflow.

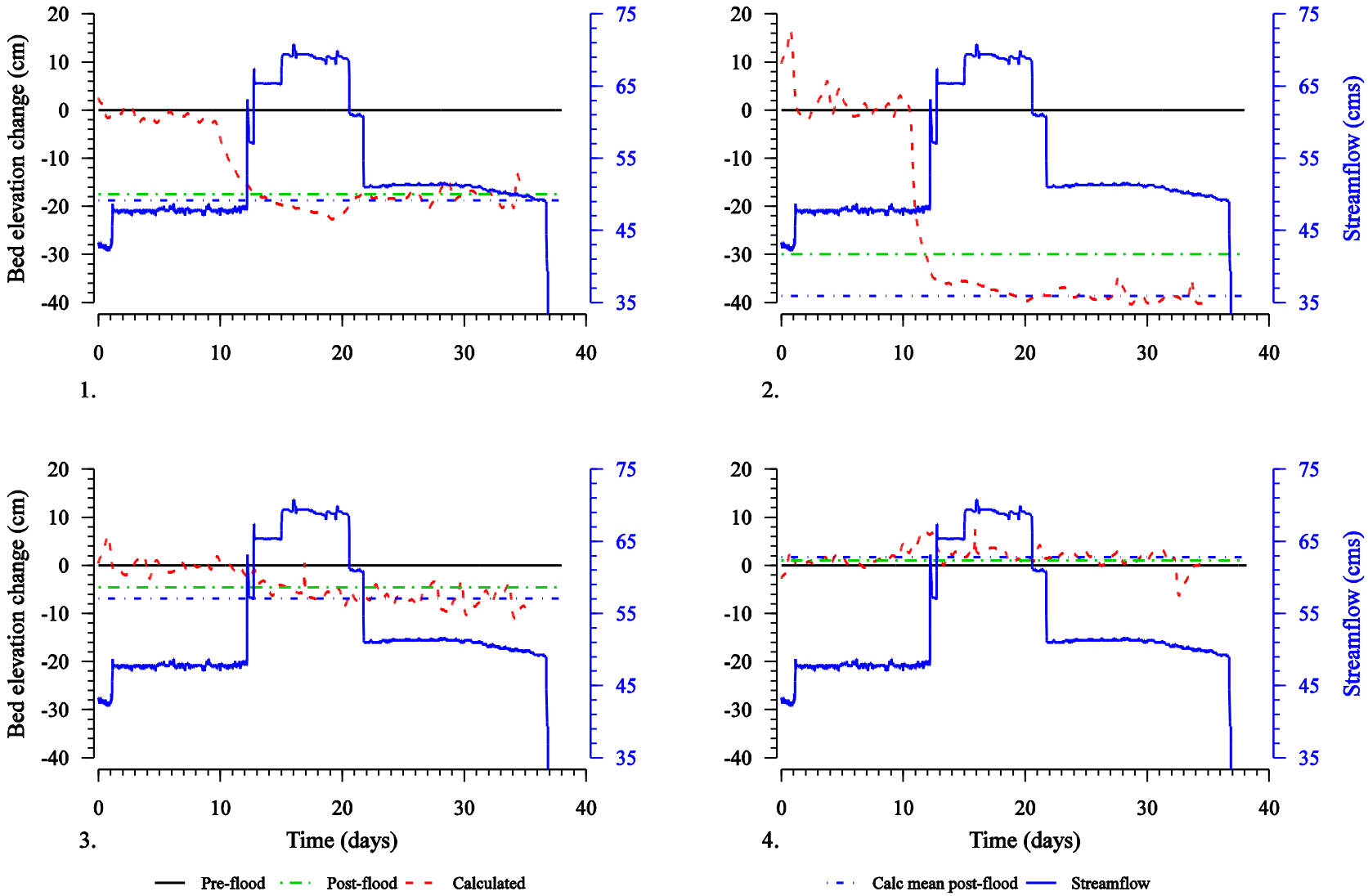

Figure 10: South Fork Boise River measured and calculated stream bed elevations at locations 1, 2, 3, and 4, plotted with the hydrograph released from Anderson Ranch Dam (secondary y-axis, blue line).

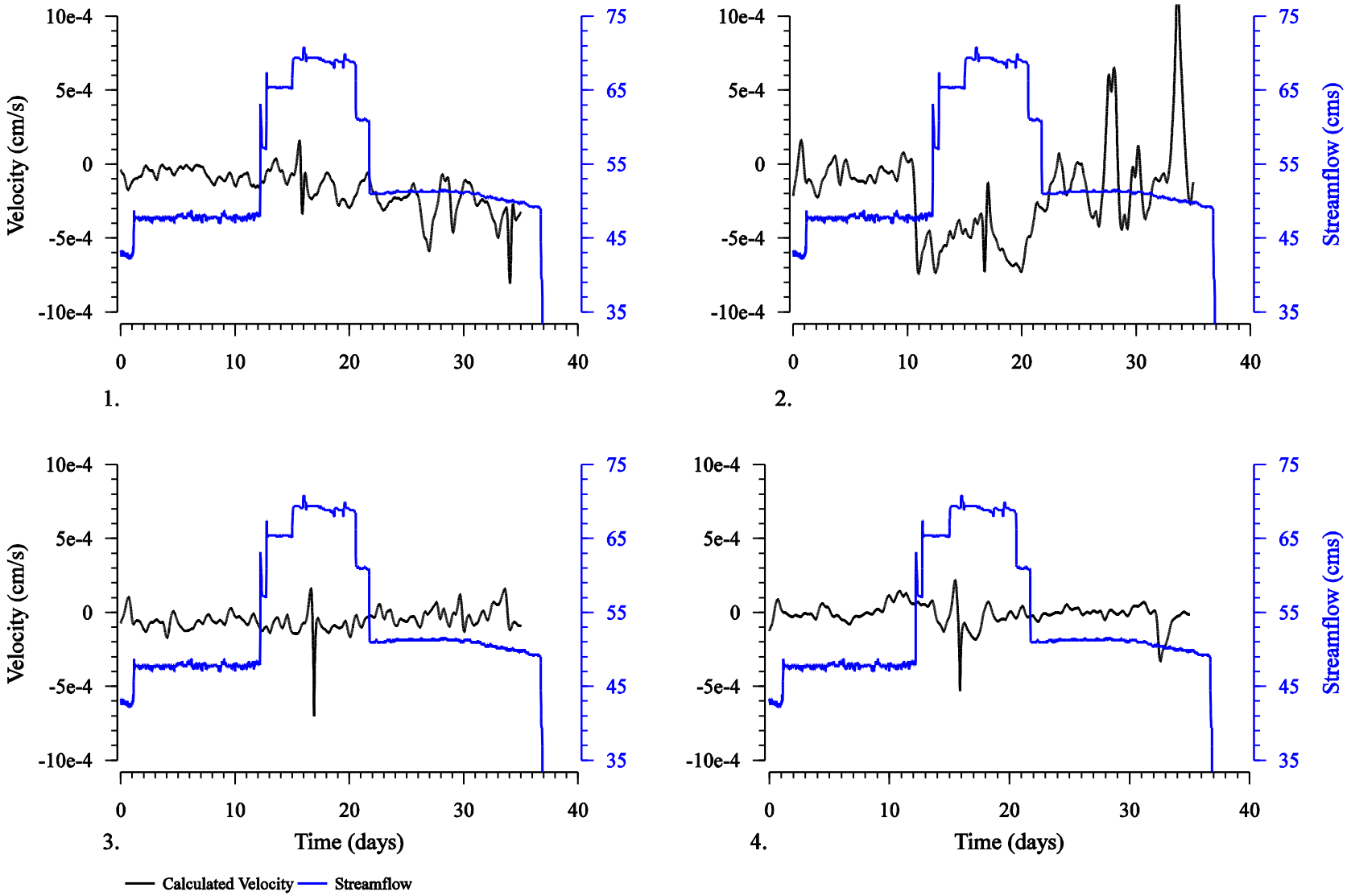

Figure 11: South Fork Boise River calculated sediment seepage velocities at field locations 1, 2, 3, and 4, plotted with the hydrograph released from Anderson Ranch Dam (secondary y-axis, blue line). Depth of temperature sensor increases with increasing sensor number.

4.0 Discussion

Quantifying seepage velocity and streambed scour/deposition from temperature time series (Gariglio et al., 2013; Hatch et al., 2006; Lautz, 2012, 2010; Luce et al., 2013; Tonina et al., 2014) relies upon an implicit assumption of turbulent, well-mixed surface water. This condition ensures water temperature within the surface water is equal everywhere. Results from the sediment tank experiment provide an opportunity to demonstrate the importance of this boundary condition explicitly. Without the surface water mixing pump in place and operating, the surface water temperature in the sediment tank tends to stratify due to low turbulence. In Figure 8a, the center deposition event shows noisy and positively biased bed elevation prediction. When surface water temperature stratification is present, the water temperature just above the bed may differ from the water temperature at the sensor used for the calculation. Phase extractions from stratified temperature surface water show difference in phase from sensors within the surface water (Figure 6). Sediment thickness calculations will then reflect non-existent sediment at this location, giving false bed change results. This boundary condition thus has implications for applications of TSDC in deep pools where stratification of surface water temperature may be present.

Bed elevation change calculations from both the laboratory and field data consistently predict scour and deposition events prior to actual occurrence of the respective event. This early prediction is due to the DFT window length parameter used in the numerical analysis. To extract phase and amplitude from any one point in the time series, the DFT function looks forward in time one discrete window length to obtain the amplitude and phase information for calculation. Increasing the window length to 4 cycles results in earlier predictions and

increased smoothing of scour/deposition events. Present analyses use window length of 2 cycles resulting in a plot predicting scour or deposition events early by 4 hours in the laboratory. A correction can be applied by adjusting calculated results back to the appropriate timing by the 2 cycles, but was not applied here to highlight the smearing effect associate with a size of a sampling window.

Window length is important when attempting to monitor live scour/deposition. For field analysis, window length of 2 cycles is 2 days, thus onset of scour is predicted 2 days of temperature data are required to obtain scour measurements. When applying this methodology to near real time monitoring of scour, it takes 2 days to obtain enough data for scour measurements. Future enhancements of this methodology might include a low resolution (depending on spacing of temperature sensors) scour alarm that can pick up differences or similarities in temperature readings from each sensor to indicate presence of sediment. Other improvements may include improved phase and amplitude extraction techniques reducing the forward, or backward depending on the adopted numerical technique, period of record necessary to perform calculations.

Laboratory bed elevation results are within RMSE of 4 mm (+/- 2 mm) for values obtained from near surface (<20 cm depth) temperature sensors. With largest particle grain sizes of the sediment tank substrate near 2 mm, this is the best possible result to be expected as actual bed elevations cannot be measured more accurately than the substrate size. As sensor depth increases, RMSE increases, and is attributed to temperature signal attenuation with depth. As the signal gets weaker, the error will increase due to increased noise in the results. Comparison of experiments B, C, and D illustrates this connection. Experiments B and C

move from high velocity to low and from sinusoidal signal to sawtooth, yet the RMSEs are similar, suggesting that signal type and velocity have little negative influence on bed measurement results. In experiment D, there is more noise, visually evident in Figure 7D and numerically with higher RMSE. Noted in Table 1, the signal amplitude for experiment D is 4 degrees Celsius versus 8 degrees Celsius in experiments B and C. Lower amplitude in experiment D leads to more noise in the calculated bed results. This degradation of the performance of the model with amplitude is expected from the analysis of propagation of error shown by Luce et al. (2013). However, filtering the noise with a moving average from experiment D bed calculations would reveal similar results to experiments B and C.

Research by others explored sensitivity of seepage velocity calculations to non-sinusoidal temperature time series (Lautz, 2012, 2010), demonstrating increased error in velocity calculations due to non-sinusoidal signals. Because the TSDC is based upon the same governing equations, it was important to consider implications of non-sinusoidal signals on monitored scour/deposition sequences in the laboratory. However, methods used by other researchers evaluate temperature time series using amplitude and phase, separately (Hatch et al., 2006; Keery et al., 2007; Lautz, 2010; Rau et al., 2012). Here, phase and amplitude are used concurrently (Gariglio et al., 2013; Luce et al., 2013; Tonina et al., 2014), which may reduce impact on results due to non-sinusoidal signals. From the present analysis, calculated bed elevations and velocities from the laboratory sediment tank show no apparent differences linked to signal type. Slightly higher error was evident during a sawtooth signal experiment but is due to a lower amplitude temperature signal. The DFT method used for calculation requires only a cyclic signal that has some measureable amplitude and consistent cycle period. Though the sawtooth signal is asymmetric, these two requirements are present, thus calculated

results are similar, and non-sinusoidal signals provide no apparent complications with this application of the TSDC.

Measured water temperature shows a vertical temperature gradient in both field and laboratory experiments (Figure 6 and Figure 9). Vertical thermal gradient has the potential to generate errors in the calculations (Lautz, 2010) because it does not honor the boundary condition of zero temperature gradients at the lower boundary. Results show accurate predictions of scour and deposition in the presence of vertical gradients, consequently this other assumption may have secondary effects (Lautz, 2010).

SFBR bed elevation change calculations show excellent utility of the TSDC in live streams. Bed changes at locations 1, 3, and 4 compare very well with physically measured values, including a range of scour and deposition. The level of accuracy in these locations is on par with other streambed surveying techniques. Conversely, field location 2 revealed significant error in calculated bed elevation change, which may be linked to grain size. In cobble and larger streambeds, it can be difficult to measure a specific bed elevation at any one location. This condition is true whether using traditional surveying methods or more advanced techniques. Grain size at this location ranged from 5 to 10 cm after scour and is comparable to the calculated error. The error in calculated scour at field location 2 may actually be due the physically measured scour used for comparison. Similarly, slight errors at the other locations may also be linked to the physical measurement. Temporal or spatial variation in effective κ_e could explain bed change calculation errors, but scour results using spatial values versus one average value yield similar results, and values calculated from adjacent paired temperature sensors before and after scour show no significant change. These analyses suggest that κ_e had

little, but likely some contribution to bed change calculation errors at any location, including location 2.

Timing and location of sediment transport events related to flow release can impact fish habitat, benthic organisms, and vegetation communities (Graf, 2006; Knighton, 1998, pp. 307–312; Ligon et al., 1995; Petts and Gurnell, 2005). Field results demonstrate the TSDC is capable of tracking timing of scour/deposition related to the dam release hydrograph (Figure 10). Considering the window length of 2 days between predicted scour and onset of high flow, each probe location properly shows scour at the onset of high flow, followed by scour rate reduction during the remaining high flow period due to larger immobile grain sizes deeper in the bed. Field site hydraulic characteristics are such that erosion is likely on the upstream end of the debris fan, while little to no erosion or deposition is expected on the downstream end. Measured and calculated erosion and deposition agree with this expectation, which helps verify success of the sediment flushing goals of the flow regime managed by USBR.

Close proximity to the dam resulted in the low amplitude, non-sinusoidal temperature signals shown in Figure 9. The signals also have strong gradients of mean with depth. The non-sinusoidal nature of the signals and changing mean with depth violate the assumptions presented by others. Consistent inaccurate calculations of scour and deposition at all locations would suggest that violation of these assumptions limits applicability of the method under these conditions, but this is not the case. Despite low amplitude and non-sinusoidal signals, results were still within desired accuracy. This suggests that the method can be used with low amplitude and/or non-sinusoidal temperature signals, which may be present in highly vegetated and shaded areas, as well as dam release reaches.

Imposed velocities in laboratory experiments were selected to demonstrate utility of the TSDC under an expected range of streambed seepage velocities (Briggs et al., 2012; Constantz et al., 2002; Gariglio et al., 2013; Keery et al., 2007; Kennedy et al., 2009). Laboratory velocity errors are similar among both sinusoidal and sawtooth signal types and the respective velocity magnitudes. High percent error in velocity results for experiments A and C are expected due to the extremely low velocity and absolute errors similar to the velocity itself. Percent error in all calculated velocities reduces with depth (Figure 8). Each velocity result for the respective temperature sensor location represents the mean velocity from the water surface to that sensor location. Preferential flows likely exist near the sides of the sediment tank, and velocities in these locations may be faster than velocities in the center. In addition, hydraulic conductivity likely varies with depth of sediment in the tank due to compaction that occurred during manual scour/deposition sequences. The deepest measurement (~10 cm from the bottom of the sediment tank) will better account for the preferential flows or variable hydraulic conductivity, where the average velocity through the entire bed is best represented. Velocity results calculated from experiments B and D at this bottom location are closest to the measured velocity, which is in fact the average velocity through the entire system. If signal penetration during experiments A and C was higher, it is likely similar error results would have been calculated from deeper temperature data.

Seepage velocities were also calculated from the field study temperature data. Locations 1 and 2 experienced significant bed scour, and changes in seepage velocities were measured after the scour event. Negative velocities indicate upward flow, which may be present at location A due to the stream receiving groundwater inputs in the area associated with steep, high ridges on either side of the river. It is possible that the small, cohesive particles present prior to scour

caused low hydraulic conductivity of the bed material, limiting the stream recharge. During scour, fine particles where removed from the surficial layer, typically 2 median grain sizes thick. The reduction of fine material in the armored layer increased the hydraulic conductivity of the sediment and thus increased seepage flux within this thin and near surface layer. At location 2, significant upward seepage flux occurred during scour, which may be linked to hyporheic return flow through the riffle from the upstream pool. Probes 3 and 4 detected little or no change in velocity after the high flow event, which is expected due to minor streambed changes at these locations. Velocity data combined with water thermal regime are useful information to characterize benthic organism habitats. Solutes and particle drift depend on near bed and intra gravel velocity, and metabolic rate and growth depend on water temperatures. Dam operations, which impact both thermal and flow regime of the surface water, affect the subsurface environment and the behavior of dwelling organisms, as observed by others (Bruno et al., 2009).

While the TSDC field application focused on erosion/deposition processes due specifically to controlled dam releases, many other potential applications are available for the method. Bed elevation changes can be measured anywhere sediment transport is expected with a temperature signal in the surface water. This tool could be useful in researching scour impacts on spawning beds and benthic organisms, whose habitats are within mobile sediments. River restoration projects could be monitored, where streambed elevation aggradation or reduction may be designed into the project or to verify erosion reduction in locations engineered for the purpose. Instream infrastructure can also be monitored for catastrophic scour, such as bridge piers to reduce costly structural damage or public safety hazards.

5.0 Conclusion

Laboratory experiments demonstrate capability of the thermal scour-deposition chain, TSDC, to quantify streambed elevation changes with millimeter accuracy in sand bed systems under the magnitudes of vertical seepage velocities studied. This capability holds true for non-sinusoidal temperature signals and with vertical thermal gradients. Differences between imposed and calculated seepage velocities are larger than those between measured and calculated streambed elevations. This is because imposed seepage velocities are the mean velocity at the sediment tank scale, whereas those calculated by the TSDC are local mean velocities between the sediment surface and the temperature sensor, thus is a scaling issue rather than uncertainty in the model estimations.

The method works under high-flow conditions in natural rivers with turbulent surface water and mixed sand and gravel beds. This holds true even for weak temperature signals (<1 degree C/day) that can occur near bottom-release dam outlets. Bed erosion calculated at the South Fork Boise River field study site is within 2 cm of actual measured values and is comparable to the bed roughness. Timing of the erosion events and streambed seepage velocity changes align with sediment flushing flows released from the upstream reservoir when the time shift due to the implemented discrete Fourier transform, DFT, is considered.

A limitation of the method has been identified in the technique for extracting the phase and amplitude from the temperature signal. The adopted DFT based on a 2-day window anticipates the timing of streambed changes within 2 cycles. This also has the effect of averaging the erosion event over a time period longer than actually occurred. Much of the uncertainty in calculated streambed changes is due to the window length rather than the

analytical solutions and occurs during the transient processes. Overall, the bed measurement accuracy of TSDC method is comparable to other bed measurement techniques.

Using temperature as a tracer provides a robust and economical method for monitoring erosion and deposition in streams, leading to application of the TSDC method for dam operation monitoring and several other applications for both engineering and ecological purposes. Bridge pier scour can be monitored in near real time, providing opportunity to reduce infrastructure catastrophic failure and potential public safety hazards. Measuring surface water and sediment temperature profiles also provides opportunities to obtain important ecological data. These data allow calculation of surface-subsurface flux to quantify gains and losses in streams, in addition to sediment thermal regime, beneficial in understanding benthic organism habitats.

References

Briggs, M.A., Lautz, L.K., McKenzie, J.M., Gordon, R.P., Hare, D.K., 2012. Using high-resolution distributed temperature sensing to quantify spatial and temporal variability in vertical hyporheic flux. Water Resour. Res. 48, W02527. doi:10.1029/2011WR011227

Bruno, M.C., Maiolini, B., Carolli, M., Silveri, L., 2009. Impact of hydropeaking on hyporheic invertebrates in an Alpine stream (Trentino, Italy). Ann. Limnol. - Int. J. Limnol. 45, 157–170. doi:10.1051/limn/2009018

Constantz, J., 1998. Interaction between stream temperature, streamflow, and groundwater exchanges in alpine streams. Water Resour. Res. 34, 1609–1615. doi:10.1029/98WR00998

Constantz, J., Stewart, A.E., Niswonger, R., Sarma, L., 2002. Analysis of temperature profiles for investigating stream losses beneath ephemeral channels. Water Resour. Res. 38, 1316. doi:10.1029/2001WR001221

Cooper, T., Chen, H., Lyn, D., Rao, A., Altschaeffl, A., 2000. A Field Study of Scour Monitoring Devices for Indiana Streams. Jt. Transp. Res. Program 2.

Deng, L., Cai, C.S., 2009. Bridge scour: Prediction, modeling, monitoring, and countermeasures—Review. Pract. Period. Struct. Des. Constr.

Gariglio, F.P., Tonina, D., Luce, C.H., 2013. Spatiotemporal variability of hyporheic exchange through a pool-riffle-pool sequence. Water Resour. Res. 49, 7185–7204. doi:10.1002/wrcr.20419

Graf, W.L., 2006. Downstream hydrologic and geomorphic effects of large dams on American rivers. Geomorphology, 37th Binghamton Geomorphology Symposium The Human Role in Changing Fluvial Systems 79, 336–360. doi:10.1016/j.geomorph.2006.06.022

Gurnell, A.M., Bertoldi, W., Corenblit, D., 2012. Changing river channels: The roles of hydrological processes, plants and pioneer fluvial landforms in humid temperate, mixed load, gravel bed rivers. Earth-Sci. Rev. 111, 129–141. doi:10.1016/j.earscirev.2011.11.005

Hatch, C.E., Fisher, A.T., Revenaugh, J.S., Constantz, J., Ruehl, C., 2006. Quantifying surface water–groundwater interactions using time series analysis of streambed thermal records: Method development. Water Resour. Res. 42, W10410. doi:10.1029/2005WR004787

Keery, J., Binley, A., Crook, N., Smith, J.W.N., 2007. Temporal and spatial variability of groundwater–surface water fluxes: Development and application of an analytical method using temperature time series. J. Hydrol. 336, 1–16. doi:10.1016/j.jhydrol.2006.12.003

Kennedy, C.D., Genereux, D.P., Corbett, D.R., Mitasova, H., 2009. Spatial and temporal dynamics of coupled groundwater and nitrogen fluxes through a streambed in an agricultural watershed. Water Resour. Res. 45, W09401. doi:10.1029/2008WR007397

Knighton, D., 1998. Fluvial forms and processes : a new perspective. Arnold ; Oxford University Press, London; New York.

L.A. Arneson, L.W. Zevenbergen, P.F. Lagasse, P.E. Clopper, 2012. Evaluating Scour at Bridges, Fifth Edition.

Lautz, L.K., 2012. Observing temporal patterns of vertical flux through streambed sediments using time-series analysis of temperature records. J. Hydrol. 464–465, 199–215. doi:10.1016/j.jhydrol.2012.07.006

Lautz, L.K., 2010. Impacts of nonideal field conditions on vertical water velocity estimates from streambed temperature time series. Water Resour. Res. 46, W01509. doi:10.1029/2009WR007917

Ligon, F.K., Dietrich, W.E., Trush, W.J., 1995. Downstream Ecological Effects of Dams. BioScience 45, 183–192. doi:10.2307/1312557

Luce, C.H., Tonina, D., Gariglio, F., Applebee, R., 2013. Solutions for the diurnally forced advection-diffusion equation to estimate bulk fluid velocity and diffusivity in streambeds from temperature time series. Water Resour. Res. 49, 488–506. doi:10.1029/2012WR012380

Lytle, D.A., Poff, N.L., 2004. Adaptation to natural flow regimes. Trends Ecol. Evol. 19, 94–100. doi:10.1016/j.tree.2003.10.002

Manzoni, S., Crotti, G., Ballio, F., Cigada, A., Inzoli, F., Colombo, E., 2011. Bless: A fiber optic sedimeter. Flow Meas. Instrum. 22, 447–455. doi:10.1016/j.flowmeasinst.2011.06.010

Marion, A., Nikora, V., Puijalon, S., Bouma, T., Koll, K., Ballio, F., Tait, S., Zaramella, M., Sukhodolov, A., O'Hare, M., Wharton, G., Aberle, J., Tregnaghi, M., Davies, P., Nepf, H., Parker, G., Statzner, B., 2014. Aquatic interfaces: a hydrodynamic and ecological perspective. J. Hydraul. Res. 52, 744–758. doi:10.1080/00221686.2014.968887

Maturana, O., Tonina, D., McKean, J.A., Buffington, J.M., Luce, C.H., Caamaño, D., 2014. Modeling the effects of pulsed versus chronic sand inputs on salmonid spawning habitat in a low-gradient gravel-bed river. Earth Surf. Process. Landf. 39, 877–889. doi:10.1002/esp.3491

Mueller, D.S., 1998. Summary of fixed instrumentation for field measurement of scour and deposition, in: Federal Interagency Workshop, Sediment Technologies for the 21st Century, Proceedings: St. Petersburg, Fla.

Nassif, H., Ertekin, A.O., Davis, J., 2002. Evaluation of bridge scour monitoring methods. U. S. Dep. Transp. Fed. Highw. Adm. Trenton.

Newson, M.D., Newson, C.L., 2000. Geomorphology, ecology and river channel habitat: mesoscale approaches to basin-scale challenges. Prog. Phys. Geogr. 24, 195–217. doi:10.1177/030913330002400203

Petts, G.E., Gurnell, A.M., 2005. Dams and geomorphology: Research progress and future directions. Geomorphology, Dams in Geomorphology 33rd Annual Binghampton International Geomorphology Symposium 71, 27–47. doi:10.1016/j.geomorph.2004.02.015

Rau, G.C., Andersen, M.S., Acworth, R.I., 2012. Experimental investigation of the thermal time-series method for surface water-groundwater interactions. Water Resour. Res. 48, W03530. doi:10.1029/2011WR011560

Richards, K., Brasington, J., Hughes, F., 2002. Geomorphic dynamics of floodplains: ecological implications and a potential modelling strategy. Freshw. Biol. 47, 559–579. doi:10.1046/j.1365-2427.2002.00920.x

Richter, B.D., Thomas, G.A., 2007. Restoring environmental flows by modifying dam operations. Ecol. Soc. 12, 12.

Stallman, R.W., 1965. Steady one-dimensional fluid flow in a semi-infinite porous medium with sinusoidal surface temperature. J. Geophys. Res. 70, 2821–2827.

Swanson, T.E., Cardenas, M.B., 2010. Diel heat transport within the hyporheic zone of a pool-riffle-pool sequence of a losing stream and evaluation of models for fluid flux estimation using heat. Limnol. Oceanogr. 55, 1741–1754. doi:10.4319/lo.2010.55.4.1741

Tonina, D., Luce, C., Gariglio, F., 2014. Quantifying streambed deposition and scour from stream and hyporheic water temperature time series. Water Resour. Res. 50, 287–292. doi:10.1002/2013WR014567